Author(s): Dalbe, Marie-Julie & Koivisto, Juha & Vanel, Loïc & Miksic, Amandine & Ramos, Osvanny & Alava, Mikko J. & Santucci, Stéphane

Title: Repulsion and Attraction between a Pair of Cracks in a Plastic Sheet

Year: 2015

Version: Final published version

Please cite the original version:

Dalbe, Marie-Julie & Koivisto, Juha & Vanel, Loïc & Miksic, Amandine & Ramos, Osvanny & Alava, Mikko J. & Santucci, Stéphane. 2015. Repulsion and Attraction between a Pair of Cracks in a Plastic Sheet. Physical Review Letters. Volume 114, Issue 20. 205501/1-5. ISSN 0031-9007 (printed). DOI: 10.1103/physrevlett.114.205501.

Repulsion and Attraction between a Pair of Cracks in a Plastic Sheet

Marie-Julie Dalbe,[1,2] Juha Koivisto,[3] Loïc Vanel,[2] Amandine Miksic,[3] Osvanny Ramos,[2] Mikko Alava,[3] and Stéphane Santucci[1,*]

[1]Laboratoire de Physique de l'Ecole Normale Supérieure de Lyon, UMR CNRS 5672, Université de Lyon, 69364 Lyon Cedex 07, France

[2]Institut Lumière Matière, UMR5306 Université Lyon 1-CNRS, Université de Lyon, 69622 Villeurbanne, France

[3]COMP Center of Excellence, Department of Applied Physics, Aalto University, 00076 Aalto, Espoo, Finland

(Received 20 December 2014; published 20 May 2015)

We study the interaction of two collinear cracks in polymer sheets slowly growing towards each other, when submitted to uniaxial stress at a constant loading velocity. Depending on the sample's geometry—specifically, the initial distances d between the two cracks' axes and L between the cracks' tips—we observe different crack paths with, in particular, a regime where the cracks repel each other prior to being attracted. We show that the angle θ characterizing the amplitude of the repulsion—and specifically its evolution with d—depends strongly on the microscopic behavior of the material. Our results highlight the crucial role of the fracture process zone. At interaction distances larger than the process zone size, crack repulsion is controlled by the microscopic shape of the process zone tip, while at shorter distances, the overall plastic process zone screens the repulsion interaction.

DOI: 10.1103/PhysRevLett.114.205501 PACS numbers: 62.20.mm, 46.50.+a

Materials science aims at improving the strength of solids and preventing the propagation of flaws that can weaken structures and lead to catastrophic events. Thus, a better understanding of fracture mechanisms in solids is obviously of crucial importance for a safer design of civil engineering structures. A large number of studies—both experimental and theoretical—have been devoted to the simplest model case of a single crack, growing in either brittle or viscoplastic materials [1–8]. Those works have shown that dynamical instabilities and/or heterogeneities may destabilize the crack dynamics, leading to strong deviations and roughness in the crack paths [6–12].

However, one single growing defect is not always at the origin of catastrophic failures, which can also be caused by the development of a network of cracks. The stress field around the crack tip is then modified by the presence of the other cracks leading to kinked trajectories. In hierarchical fracturing processes [13], it is usually observed that cracks coalesce around a 90° angle, as for example in dessication [14–16] or in fault dynamics [17–20]. It has also been shown that two collinear approaching cracks (submitted to a uniaxial stress in mode I) can repel each other instead of merging tip to tip [21], resulting in a curved, "hook-shaped" path. Such cracks have been observed for a wide range of scales in nature, from 25 cm quartz-feldspar veins in granite to 25 km-long oceanic ridges [18], as well as in laboratory experiments on glass [22], Polymethylmethacrylate plates [21,23] or more recently in paper [24] and gelatin sheets [25]. Theoretical studies have tried to explain this truly nonintuitive behavior. First, Melin [23] showed that the collinear crack configuration is unstable. Then, Kachanov [26] noticed that the slightest disturbances in the initial symmetric configuration will give rise to a mixed mode interaction (traction and shear stresses). The fact that the cracks are observed to deviate instead of going straight to minimize shear stresses led him to suggest that the cracks might actually follow a path that maximizes the energy release rate, instead of the path following the principle of local symmetry [27,28]. Numerical simulations [29–31] can only reproduce qualitatively the shapes observed, and most of experiments have been performed only on the final post-mortem path (usually obtained in a fast dynamic fracture regime [23,24]). Finally, very few works have studied in detail, or even simply ignore the repulsive part of the fracture trajectory [25], and especially the amount of deviation, for which no clear predictions are established.

In this Letter, we present an experimental study of the interaction of two collinear cracks in a polymer film. Influence of material properties has been investigated by comparing different polymers. When submitted to uniaxial stress at a small constant loading velocity, the two cracks grow slowly towards each other, modifying the long range elastic stress field at their tips. As a result, we observe strong deviations in their paths, with in particular a regime where the cracks repel each other, which depends on the initial distances separating the two cracks—d between the two cracks' axes and L between the cracks' tips. We show that the angle θ characterizing the amplitude of the repulsion—and specifically its evolution with d—depends strongly on the material used, and in particular, on the microscopic shape of the fracture process zone. This process zone—even when it is microscopic—can strongly modify the structure and

intensity of the singular stress field ahead of the crack tip, and as a consequence, the interacting crack trajectories.

We have used different types of samples: polyester (PET) sheets (Mylar®, and Lumirror®), and polycarbonate (PC) sheets. The PET samples are 190 μm thick, and have a dimension of 80×100 mm^2, so that when they are clamped, the actual area of study is a square of 80×80 mm^2. The PC sheets are slightly larger, so that the area of study is 100×100 mm^2. Moreover, we used two different sets of PC sheets with a thickness $e = 125$ and 250 μm. The experiments were performed at a temperature of 21 ± 1 °C and a humidity of $40\% \pm 5\%$. We prepared two initial notches, symmetric to the center of the sample, separated by a distance d vertically and L horizontally. We have varied systematically these two parameters, so that $0 < d < 4$ cm and $1 < L < 6$ cm. The samples clamped in a tensile testing machine are pulled from one side at a fixed velocity $v = 0.02$ mm s^{-1}, while the other side is fixed [Fig. 1(a)]. This is done in a uniaxial plane stress loading (lateral sides free to move). Using a standard digital camera recording two pictures per second, we directly follow and observe the slow growth of the pair of cracks. Because of the long range elastic field, each crack modifies the stress field at the tip of its opposing crack, except at the early stage of the experiments when the two cracks can be relatively far apart. As a result, the two cracks interact with each other, and their trajectories do not stay perpendicular to the applied stress. In Figs. 1(b) and (c),

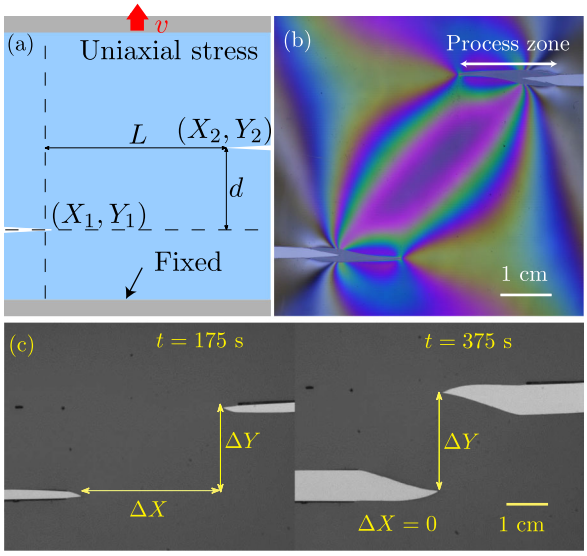

FIG. 1 (color online). (a) Schematic representation of the experiments. A plastic sheet with two initial notches separated by vertical d and horizontal L distances is submitted to a mode I loading at a constant imposed velocity. We follow the slow interacting growth of the two cracks, with for instance (b) $d = 2$ cm and $L = 4$ cm, in PC samples (close-up), with photoelasticity; or (c) PET Mylar® sheets (close-up) at two different times.

we show typical images recorded during experiments performed on PET Mylar® and PC samples, which, unlike PET, display a macroscopic flame-shaped process zone where the sheet thins [5]. Under stress, these materials become birefringent. Thus, it is easy to at least observe and characterize qualitatively how the stress field is modified by the presence of another defect, by placing the sheets in between two polarizers [32]. In Fig. 1(b), we observe the specific patterns of isochromatic fringes (showing zones of constant principal stress differences) due to the interaction between the cracks and their process zones in PC films.

We present first results for a set of experiments performed on PET Mylar® sheets. Young's modulus of those samples is $E = 1.8 \pm 0.1$ GPa. The maximum force measured in those experiments is approximately 800 N, corresponding to an elongation of 0.24 cm. Analyzing the images typically recorded during an experiment [as the one shown in Fig. 1(c)], we detect the crack tips' coordinates (X_1, Y_1) and (X_2, Y_2). To characterize the interacting cracks' trajectories, we consider the relative positions $\Delta X = X_2 - X_1$ and $\Delta Y = Y_2 - Y_1$ corresponding to the horizontal and vertical distances between the two crack tips (Fig. 1). It is important to minimize the contribution of the elastic tensile elongation Δv of the samples on the distances measured in the deformed state. We thus consider the quantity $\Delta y = \Delta Y - \Delta Y_m$, with $\Delta Y_m = d + \Delta v$ the measured distance between the axes of the two cracks in the deformed state. We don't analyze our experiments when the sample starts to go out of plane, which typically occurs when the cracks overlap, i.e., $\Delta X \approx 0$ cm.

We study the evolution of this relative vertical distance between the cracks Δy as a function of the horizontal crack separation ΔX for the various initial geometrical conditions. We usually observe that when ΔX decreases (which corresponds to the time increasing), Δy first increases: the two cracks repel each other. Then, Δy reaches a maximum at a point $(\Delta X_t, \Delta y_t)$ and finally decreases: the two cracks attract each other. In Fig. 2(a), we study this typical behavior for a fixed initial vertical crack distance $d = 2$ cm and different initial horizontal crack separation L, for PET Mylar® samples. In order to compare quantitatively the various experimental conditions, we shift the trajectories using the turning point as the origin, plotting $\Delta y - \Delta y_t$ vs $\Delta X - \Delta X_t$. Interestingly, we observe that the various trajectories collapse on a single master curve, showing that they do not depend on L. For PET Mylar® samples, the repulsive regime is observed in a given range of scales $1 \leq L \leq 5$ cm, while when L is larger no interaction is observed. In Fig. 2(b), we plot Δy vs ΔX for a given L and different d for PET Mylar® sheets. In contrast to previous observations, the crack pair trajectories depend strongly on the initial vertical crack separation d, with a stronger repulsion when the initial vertical crack separation d decreases. Interestingly, we notice in Fig. 2(b) that the two cracks start to attract each other for $\Delta X > 0$ cm

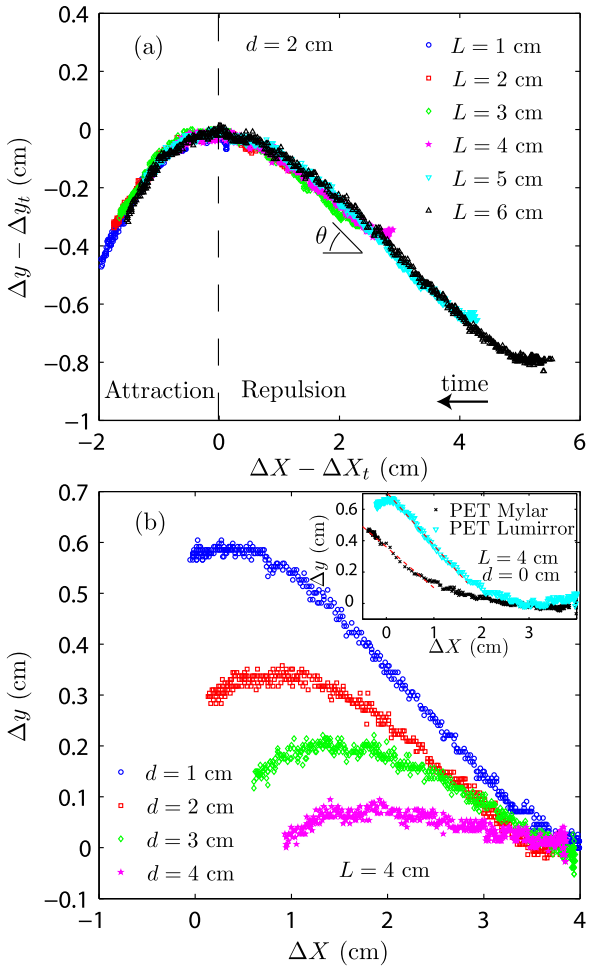

FIG. 2 (color online). Crack pair trajectories for various experimental conditions obtained with PET Mylar®. We plot in (a) $\Delta y - \Delta y_t$ vs $\Delta X - \Delta X_t$ for $d = 2$ cm, and various L. In (b), we represent $\Delta Y - d$ vs ΔX for $L = 4$ cm and various d, as well as for two different PET samples at $d = 0$ cm (inset).

with $\Delta X_t \approx d/2$. Thus, we can propose a phase diagram in the (L, d) space (in the Supplemental Material), showing when the beginning of the trajectories are attractive or repulsive for PET Mylar® sheets. Our results appear in contrast to recent observations in gelatin sheets [25], where no crack repulsion was reported, and cracks were shown to attract at $\Delta X = 0$. These observations were the justification for a geometrical model, considering solely that cracks start to attract each other when they overlap. In our various experiments, this assumption (which corresponds to $\Delta X_t = 0$) is obviously not true. We nevertheless were able to fit the attractive part of the trajectories with a parabolic shape as predicted in Ref. [25]. However, this model cannot explain the repulsive trajectories.

Therefore, we focus our study on the repulsive part of the Δy vs ΔX curves, by measuring the angle θ corresponding to the maximum slope of the crack paths shown in Fig. 2. While we have already observed in Fig. 2(a) that this

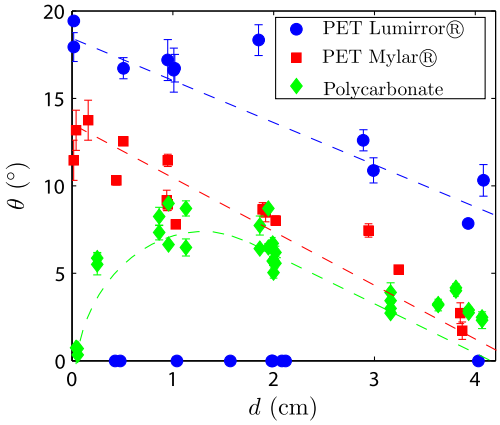

FIG. 3 (color online). Repulsion angle θ vs d for a given $L = 4$ cm (PET) or $L = 6$ cm (PC), for different types of plastic sheets. Each point represents the estimated slope for one experiment, with its fitting residual as an error bar. Lines are guides for the eye.

repulsion angle θ is independent of L, we report now its evolution with d in Fig. 3. This angle of repulsion θ decreases with d towards zero for large distance ($d \geq 4$ cm, in our geometry), meaning that, if the cracks are too far from each other, they will not feel each other and their trajectories will be straight. For the very specific and singular condition $d = 0$, we observe that the two cracks start to interact and specifically repel at different (smaller) length scales ΔX, contrary to the experiments at larger d [see inset of Fig. 2(b)]. Nevertheless, the angle θ characterizing the maximum repulsion, evolves systematically with d and is maximal for $d = 0$ cm, when the cracks are aligned with each other. Our experimental results question the validity of the principle of local symmetry [27,28] as an appropriate criterion for crack propagation. We checked that finite element analysis simulations based on this principle does not lead to the strong repulsion observed for $d = 0$. An alternative criterion for the cracks' path could be instead that the cracks grow towards the direction of maximum energy release rate, as proposed by Kachanov [26] and supported also by recent observations of wavy cracks in drying colloidal films [33].

We compare now the interaction of crack pairs in various plastic sheets. We have used a second type of polyester: transparent PET Lumirror® sheets, in contrast to the milky aspect of the PET Mylar® samples (due to the presence of titanium dioxide nanoparticles). Even though those PET samples have different visual aspects, we verified that they have the same macroscopic mechanical properties (Young's modulus and yield stress)—characterized by identical strain-stress curves.

In Fig. 3, we report first the evolution of the repulsion angle θ as a function of the initial vertical crack separation d, for a fixed horizontal distance $L = 4$ cm, for the two types of PET samples. The experiments on PET Lumirror®

sheets gave, for identical sets of geometrical parameters (d, L), two different behaviors for the interaction of the cracks: either the cracks could interact without any repulsion ($\theta = 0°$), or they repelled each other. In that case, the repulsion angle θ is systematically larger than for the Mylar® samples. The statistical behavior of the interaction of the cracks is reminiscent of recent results observed for an array of cracks in paper sheets [24], which was attributed to the heterogeneous fiber structure of those samples. Indeed, contrary to the Mylar® samples, we could notice some scratches on the surface of the Lumirror® sheets, that can introduce some heterogeneity in the mechanical response of the samples. More importantly, the fact of observing different repulsion angles in samples with identical strain-stress curves shows the limits of theoretical descriptions of the interactions of the cracks based only on linear elastic fracture mechanics. It suggests the importance of nonlinearities in the singular stress field at the crack tips. Indeed, the two PET samples present different microscopic plastic process zones with a sharper tip in Lumirror® sheets, while for Mylar® samples the larger thin plastic zone along the sides of the cracks forms a bident pitchfork at the crack tip (see Supplemental Material [34]).

Then, we studied the interaction of cracks in polycarbonate sheets (Young's modulus $E = 1.1 \pm 0.1$ GPa) which display a much larger plastic process zone. Indeed, a centimeter flame-shaped process zone develops at the crack tip during its growth [5] as already mentioned and shown in Fig. 1(b). We performed the same analysis as for the PET samples, but considering the horizontal distances ΔX_c and ΔX_{pz} as well as the vertical separations (subtracting the elastic deformation of the samples) Δy_c and Δy_{pz}, between the cracks and process zones, respectively. First of all, as in PET samples, the trajectories and more specifically, the curves ΔX vs Δy do not depend on the initial horizontal crack separation L, but evolve systematically with the vertical distance initially separating the two cracks d. Interestingly, we observed that the repulsive part of the crack pair trajectories are identical to the ones of the process zones (just delayed in time). Besides, we observed that the cracks' interactions do not depend on the thickness of the studied polycarbonates sheets. We therefore report the various values of the angle θ characterizing the early repulsion between either the two process zones or the two cracks as function of d with the same diamond symbol for those various experiments, performed at $L = 6$ cm. Interestingly, we observe that the evolution of θ is nonmonotonic, with a maximum for $d \approx 1$ cm, corresponding roughly to the width of the process zone. Compared to PET samples, the much larger process zone in PC has apparently a screening effect on the repulsive interactions between the two cracks at small d. On the contrary, at distances d larger than the characteristic process zone size, the angle of repulsion is very close to the ones measured for the PET Mylar® sheets, which probably reflects the similar double tip shape of the plastic process zone [34]. In that case, it is not the size of the process zone which seems to be relevant, but indeed, the strong similarity of the process zone tips in the two materials.

To conclude, we have presented a detailed experimental study of the interaction of two collinear cracks in various polymer films, focusing on the regime where the cracks repel each other, instead of merging tip-to-tip. We show that the angle θ characterizing the strength of the repulsion—and specifically its evolution with the initial distance d between the two cracks' axes—depends strongly on the microscopic behavior of the material considered. Indeed, for the two PET samples with similar macroscopic mechanical properties (Young's modulus, yield stress), we could observe different crack paths, with different amplitudes of crack repulsion. We relate this effect to differences in the shape of the microscopic process zone, which will affect both the intensity and structure of the stress field where the cracks will grow. The process zone tip in PET Lumirror samples is significantly sharper leading to a larger amplitude of the stress at the crack tip, and a stress field acting on a longer range. To support this claim, we performed as well a series of experiments on polycarbonate samples, for which a large flame-shape plastic process zone can be observed at the crack tip. Although the plastic process zone is much larger in PC films, the repulsion angle for large d is the same as in one of the PET samples. We relate this observation to the similar tips of the process zones at "microscopic" scale in the two materials, leading to a similar stress singularity at large enough distance from the process zone. When the distance between the cracks is too small compared to the size of the process zone in PC films, the stress field becomes very different from the one in PET, and leads to a screening of the repulsion between the cracks. In that case, the amplitude of the deviation between the cracks is reduced and even cancels for small values of d, reflecting the screening effect of the large process zone. Therefore, we can indeed suggest that the repulsion between cracks (that could be related to a path maximizing the energy release rate [26]) depends strongly on the intensity of the stress field at the crack tips. The significance of our results is obvious if one considers the fact that most materials–if not all–do exhibit ductile behavior and a fracture process zone at the crack tips [35]. Our experimental results call for new theoretical approaches where such an effect needs to be taken into account in order to develop an appropriate theory of interacting cracks.

We thank S. Roux, V. Lazarus, and J. Mathiesen for invaluable discussions. S. Santucci wishes to thank the Visiting Professor Programme of the Aalto University

School of Science. We acknowledge the financial support of Ecole Normale Supérieure de Lyon and the Academy of Finland through the Centre of Excellence Program (Project No. 251748).

*stephane.santucci@ens-lyon.fr

[1] B. R. Lawn and T. R. Wilshaw, *Fracture of Brittle Solids* (Cambridge University Press, Cambridge, England, 1975).
[2] R. Schapery, Int. J. Fract. **11**, 141 (1975).
[3] M. F. Kaninnen and C. H. Popelar, *Advanced Fracture Mechanics* (Oxford University Press, New York, 1985).
[4] M. Marder and S. Gross, J. Mech. Phys. Solids **43**, 1 (1995).
[5] P.-P. Cortet, S. Santucci, L. Vanel, and S. Ciliberto, Europhys. Lett. **71**, 242 (2005).
[6] M. J. Alava, P. K. V. V. Nukala, and S. Zapperi, Adv. Phys. **55**, 349 (2006).
[7] S. Santucci, L. Vanel, and S. Ciliberto, Eur. Phys. J. Spec. Top. **146**, 341 (2007).
[8] L. Vanel, S. Ciliberto, P. Cortet, and S. Santucci, J. Phys. D **42**, 214007 (2009).
[9] N. Mallick, P.-P. Cortet, S. Santucci, S. G. Roux, and L. Vanel, Phys. Rev. Lett. **98**, 255502 (2007).
[10] D. Bonamy and E. Bouchaud, Phys. Rep. **498**, 1 (2011).
[11] J. Scheibert, C. Guerra, F. Célarié, D. Dalmas, and D. Bonamy, Phys. Rev. Lett. **104**, 045501 (2010).
[12] L. Laurson, X. Illa, S. Santucci, K. T. Tallakstad, K. J. Måløy, and M. J. Alava, Nat. Commun. **4**, 2927 (2013).
[13] S. Bohn, S. Douady, and Y. Couder, Phys. Rev. Lett. **94**, 054503 (2005).
[14] A. Groisman and E. Kaplan, Europhys. Lett. **25**, 415 (1994).
[15] S. Bohn, L. Pauchard, and Y. Couder, Phys. Rev. E **71**, 046214 (2005).
[16] Y. Cohen, J. Mathiesen, and I. Procaccia, Phys. Rev. E **79**, 046109 (2009).
[17] K. Macdonald, J.-C. Sempere, and P. J. Fox, J. Geophys. Res. **89**, 6049 (1984).
[18] D. D. Pollard and A. Aydin, J. Geophys. Res. **89**, 10017 (1984).
[19] V. Acocella, A. Gudmundsson, and R. Funiciello, J. Struct. Geol. **22**, 1233 (2000).
[20] T. Candela and F. Renard, J. Struct. Geol. **45**, 87 (2012).
[21] A. Eremenko, S. Novikov, and A. Pogorelov, J. Appl. Mech. Tech. Phys. **20**, 477 (1979).
[22] M. Swain and J. Hagan, Eng. Fract. Mech. **10**, 299 (1978).
[23] S. Melin, Int. J. Fract. **23**, 37 (1983).
[24] P.-P. Cortet, G. Huillard, L. Vanel, and S. Ciliberto, J. Stat. Mech. (2008) P10022.
[25] M. L. Fender, F. Lechenault, and K. E. Daniels, Phys. Rev. Lett. **105**, 125505 (2010).
[26] M. Kachanov, *Elastic Solids with Many Cracks and Related Problems*, Advances in Applied Mechanics Vol. 30 (Academic Press Inc, New York, 1994), pp. 259–445.
[27] F. Erdogan and G. C. Sih, ASME J. Basic Eng. **85**, 519 (1963).
[28] B. Cotterell and J. Rice, Int. J. Fract. **16**, 155 (1980).
[29] J.-C. Sempere and K. C. Macdonald, Tectonics **5**, 151 (1986).
[30] H. Chan, Eng. Fract. Mech. **39**, 433 (1991).
[31] P. Baud and T. Reuschlé, Geophys. J. Int. **130**, 460 (1997).
[32] See Supplemental Material at http://link.aps.org/supplemental/10.1103/PhysRevLett.114.205501 for a video recording that shows the interaction of two cracks in a polycarbonate sample using photoelasticity.
[33] L. Goehring, W. J. Clegg, and A. F. Routh, Soft Matter **7**, 7984 (2011).
[34] See Supplemental Material at http://link.aps.org/supplemental/10.1103/PhysRevLett.114.205501 where we show microscopic images of the cracks and plastic process zones tips for the various samples studied.
[35] F. Célarié, S. Prades, D. Bonamy, L. Ferrero, E. Bouchaud, C. Guillot, and C. Marlière, Phys. Rev. Lett. **90**, 075504 (2003).